Ultrafast X-ray Diffraction of Photodissociation of Iodoform in Solution

Jae Hyuk Lee[†], Tae Kyu Kim[†], Joonghan Kim[†], Maciej Lorenc[¶], Qingyu Kong[¶], Michael Wulff[¶], and Hyotcherl Ihee[†*]

[†]*Department of Chemistry and School of Molecular Science (BK21), Korea Advanced Institute of Science and Technology (KAIST), Daejeon, 305-701, Republic of Korea*
[¶]*European Synchrotron Radiation Facility, Grenoble Cedex 38043, BP 220, France*

Abstract. We studied structural dynamics in the photodissociation of iodoform (CHI_3) dissolved in methanol by time-resolved x-ray diffraction. A femtosecond laser pulse induces the bond-breaking of an iodine atom from iodoform and an x-ray pulse generated from a synchrotron gives time-dependent diffraction signal which contains the structural information of photoproducts with 100 ps time-resolution and 0.001 Å spatial resolution. CHI_2 radical and I atom are formed by the results of the ultrafast photodissociation of iodoform and these intermediates recombine to form iodoform again via geminate recombination. The iodine atoms which escape from the cages nongeminately recombine to form I_2. Solvent dynamics, heating and solvent expansion, caused by photodissociation, are also explained from time-resolved x-ray diffraction data.

Keywords: Time-resolved solution x-ray diffraction, CHI_3, Hydrodynamics
PACS: 82.53.Uv, 61.10.Eq

INTRODUCTION

Through the advancement of computational methods, the prediction of transient molecular structure during chemical/biological reactions has become relatively easy. In contrast, direct experimental visualization of temporally varying transient structures during ultrafast processes has been recently performed with great technical advances, but it is still difficult [1]. Recent advancements have been achieved in time-resolved optical spectroscopy to correlate frequencies of optical transition of molecules with temporal behavior of molecular structure. Since the optical probe is not able to interfere with all atoms, structural changes of transient species can not be obtained directly, but have to be deduced from potential energy surfaces of molecular species. In this regards, the methodology of time-resolved x-ray diffraction [2-5], in which structural information can be obtained from the diffraction patterns, offers a complementary tool. The reaction is triggered optically as in the conventional spectroscopy, but relevant reactions are probed by the diffraction of ultrashort x-ray pulses. The wavelength of x-ray is typically less than 1 Å and x-ray can track the motions of each atom in the liquid phase. Time-resolved x-ray absorption spectroscopy must also be mentioned as a complementary atomic probe to time-resolved x-ray diffraction [6].

The proof of principle for liquid phase time-resolved diffraction experiments with 100 ps time resolution has been published previously [2-4]. In these works, experimental determination of temporally varying atom-atom pair distribution functions has been achieved. More recently, rather complex structural dynamics of $C_2H_4I_2$ dissolved in methanol has been elucidated [4]. In this approach, the changes in scattering due to photoexcitation were considered as several classes of diffraction modifications: (i) the structural changes in the solutes by the photoreaction, (ii) the changes of solvent cage structure around solute molecules, and (iii) the solvent's structural change due to the energy transfer (such as heating and thermal expansion). The hydrodynamics of the solvents are mathematically correlated with time-dependent solution reaction dynamics, which can transfer energy from photon-absorbing solute molecules

---

[*] Author to whom correspondence should be addressed. E-mail: Hyotcherl.Ihee@kaist.ac.kr

to the solvent. In the present study, we have investigated structural dynamics of iodoform in methanol solution using synchrotron based time-resolved liquid phase x-ray diffraction.

Following excitation of a nonbonding electron localized on C-I bond to an antibonding ($n(I) \rightarrow \sigma^*$(C-I) transition), one of the C-I bond in the iodoform is broken [7]. As results, the iodine atom, which is formed in the cage may escape from the cage, or it may recombine geminately with CHI_2 radical to produce the parent molecule or isomer configuration of iodoform, iso-iodoform (CHI_2-I). Recent investigations using transient resonance Raman spectroscopy and femtosecond pump-probe spectroscopy have shown that initially produced photofragments, iodine atom and CHI_2 radical, recombine within the solvent cage to form the isomer of CHI_2-I and the isomer is stable in the cage up to μs range.[7-8] However, direct evidence of isomer formation can be provided only by using time-resolved x-ray diffraction. Here we determined the primary reaction pathway and subsequent structural dynamics of dissociated CHI_3 in methanol using time-resolved x-ray diffraction. The difference diffraction data were analyzing globally by considering the diffraction contributions from solute, cage, and solvent's hydrodynamic responses.

EXPERIMENTAL

Time-resolved diffraction data were collected on the beamline ID09B at the European Synchrotron Radiation Facility (ESRF) using the optical-pump and x-ray-probe scheme. The detailed experimental geometry and analysis procedure were previously described [2-4]. In brief, 20 mM CHI_3 (Aldrich, 99.5%) was circulated through a high pressure sapphire slit nozzle (300 μm thickness and 1-5 m/s jet speed). Femtosecond laser pulses from a Ti:Sapphire laser system, synchronized with the single pulse of x-ray, were frequency tripled and temporally stretched to 2 ps to avoid multiphoton excitation. After electronically setting the time-delay (~3 ps accuracy), polychromatic x-ray pulses (5×10^8 photons per 100-ps-long pulse, ~ 3% of $\Delta E/E$) were focused onto the sample jet (100×60 μm^2 spot size). Scattering of x-ray from the sample were collected with an area detector (MARCCD) with a sample-to-detector distance of 43 mm. The diffraction data were averaged over 20 images and were normalized to the total scattering in the region $6.84 \leq q \leq 6.99$ Å^{-1} where the scattering is insensitive to structural changes. Diffraction data were measured for time-delays of -200 ps, 100 ps, 300 ps, 1 ns, 3 ns, 6 ns, 10 ns, 30 ns, 45 ns, 60 ns, 300 ns, 600 ns, 1μs, and 3 μs. Additional time-delay (-3 ns) was also collected between the images. Difference-diffraction curves ($\Delta S(q,t)$, [$q=(4\pi/\lambda)\sin(2\theta/2)$ where λ is the wavelength of the x-rays and θ is the scattering angle; t is the time delay]) were generated by subtracting the reference data at -3 ns from the data at any other time-delay.

RESULTS AND DISCUSSION

General Information from Difference Diffraction Intensity

The difference diffraction intensities ($q\Delta S(q,t)$) and related radial distribution functions $r\Delta S(r,t)$ are shown in Fig. 1(A) and (B). At -100 ps, which referenced to the time-delay of -3 ns, there is no difference diffraction intensity as expected. At positive time-delays, the difference diffraction patterns emerge and progress with time. More direct information of structural changes can be drawn in the real-space representation of the difference diffraction intensity, $q\Delta S(q,t)$. The sine-Fourier transformation of $q\Delta S(q,t)$ provides one way of the real-space representation, $q\Delta S(q,t)$:

$$r\Delta S(r) = \frac{1}{2\pi^2} \int_0^\infty q\Delta S(q)\sin(qr)\exp(-kq^2)dq \qquad (1)$$

where the constant k (k=0.03 Å^2) is a damping constant. This difference radial distribution function (RDF), $r\Delta S(r,t)$ is resulted from the average electron density changes by the illumination as a function of interatomic distance, r. Since iodine scatters x-ray more than the other atoms (C, H, and O) in this molecular system, the structural changes of iodine-iodine distance are much pronounced in this representation. The RDFs in Fig. 1(B) exhibit both negative and positive peaks: there is strong depletion of correlation at 3.8 Å with a corresponding rise at 2.9 Å at early times. Since the structural parameters of CHI_3 are well known [8], one can easily assign the negative peak to the bond breakage of C-I in CHI_3 and positive peak to the formation of new C-I bond in CHI_2 radical. However the detailed analysis must include all three contributions: solute-solute, solute-solvent and solvent-solvent which is done in the following section [4,5].
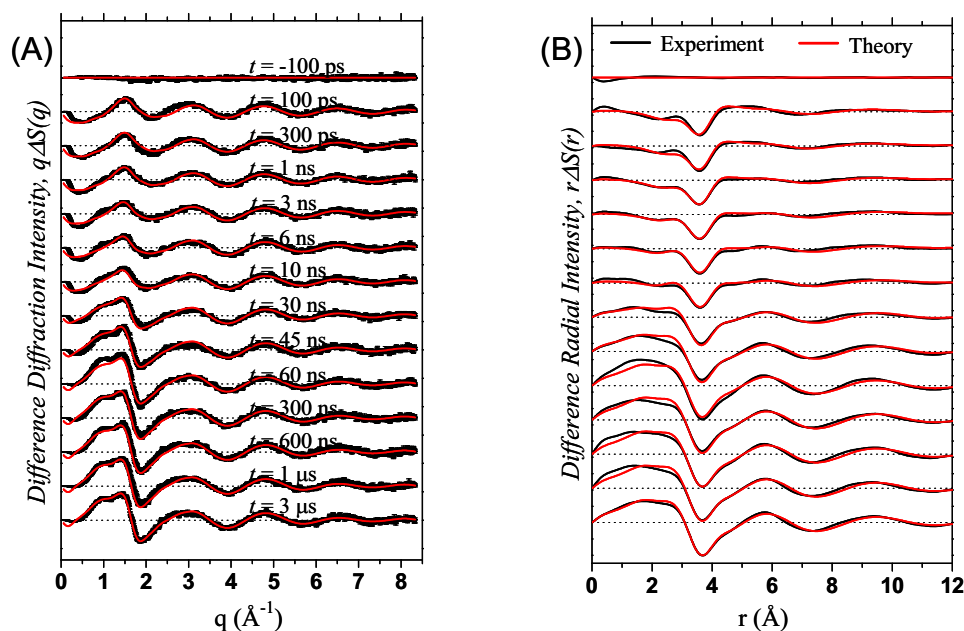
1263

FIGURE 1. Time-resolved diffraction signal for CHI_3 in methanol. (A) Difference diffraction intensities (black), $q\Delta S(q,t)$, excited minus nonexcited. (B) Difference radial distribution functions (black), $r\Delta S(r,t)$ which are sine-Fourier transforms of $q\Delta S(q,t)$ in (A). In both figures, the best fits from a theoretical model are also shown in red curves.

Global Fitting of Difference Diffraction Patterns

To explain and fit the experimental difference diffraction ($q\Delta S(q,t)$), we include all three contributions (solute, solute-solvent cage, solvent's responses). For the solute contribution, we considered all photoreaction pathways. Following photoexcitation, the parent molecules (CHI_3) are dissociated to the CHI_2 and I radicals. These radicals can recombine to the parent molecule (CHI_3) or to the isomer (CHI_2-I). Moreover, the I radical can escape from the cage and recombine to I_2 with I radical from the other cage or make CHI_3 again via nongeminate recombination. In summary, we have five different solute candidates (CHI_3, CHI_2, CHI_2-I, I, and I_2).[7,8] Theoretical scattering curves of these photo-species, which contain the solute and solute-solvent cage structures, were obtained from molecular dynamics (MD) simulations. The pure solvent's contribution is originated from heating and subsequent thermal expansion. Heating is induced by the transfer of energy from the photon-absorbing solutes to the surrounding solvent. Recently we showed that these hydrodynamic effects, i.e. the solvent response to an ultrafast temperature rise ($[\partial S(q,t)/\partial T]_\rho$ and $[\partial S(q,t)/\partial \rho]_T$), can be determined experimentally in pure methanol, without inducing any chemical change, by exciting it with near IR laser pulses that excite over-tones in C-H and O-H vibrations [9].

Once we have obtained all components, the experimental difference diffraction data were fit with a linear combination of these components. The basis set of model functions consists of the solvent terms ($[\partial S(q,t)/\partial T]_\rho$ and $[\partial S(q,t)/\partial \rho]_T$), the difference scattering functions from transitions in the solutes alone, and their caged equivalents. Since hydrodynamic changes (temperature and density changes) of the solvent is mathematically linked by solute reaction dynamics, i.e. time-dependent solute concentration changes, the data of all time-delays are linked and were fitted globally instead of fitting the data at each time-delay separately. The fitting parameters include the reaction constants of all solute chemical reactions, the laser spot size and yields of photodissociation and vibrational cooling processes. As results, this global-fitting process produces time-dependent concentration changes of all putative solute species, and time-dependent temperature and density changes of bulk solvent. More detailed descriptions of global-fitting method can be found in elsewhere [4]. Optimal fits to all experimental data using a kinetic model for $CHI_3 \rightarrow CHI_2 + I$ and subsequent reactions are shown in Figs. 1(A) and 1(B). The fitted theoretical curves successfully reproduce experimental difference curves. The resulting reaction dynamics of solute and hydrodynamics changes of bulk solvent are shown in Fig. 2(A) and 2(B), respectively.
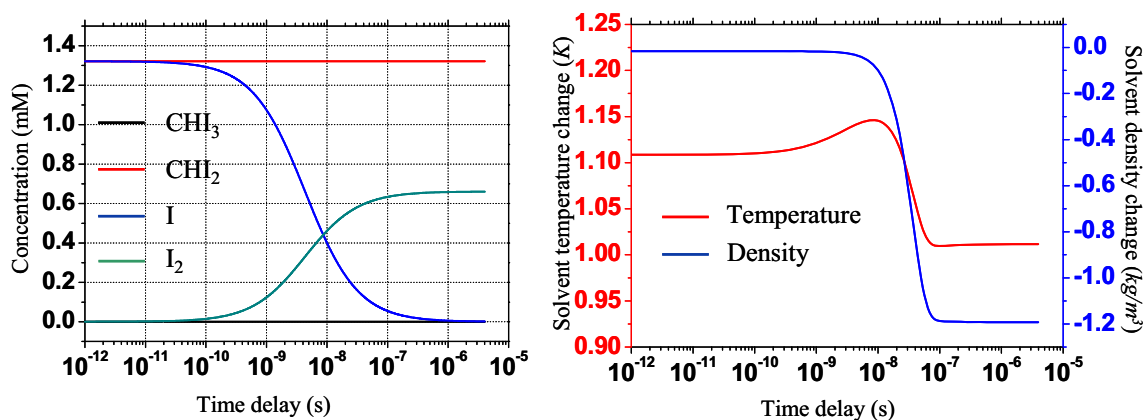
1264

FIGURE 2. (A) The population change of the all photo-species as a function of time-delay. (B) The changes in the solvent temperature (red) and density (black) as a function of time-delay.

Structural Dynamics of Photoreaction of Iodoform

Figure 2(A) shows the population changes of all related chemical species from the global fitting. CHI_2 and I are the dominant species at 100 ps and they originate from prompt dissociation of the parent molecules in the cage. Then most of I radicals recombine non-geminately with iodine atoms that have escaped from another solvent cages to form the I_2 molecules with the rate constant 3.1 (± 0.5) $\times 10^{10}$ $M^{-1}s^{-1}$. The time constant for the non-geminate recombination of I_2 is close to the values found in CCl_4 solutions from optical spectroscopy [10]. After thermal expansion, the density of the solvent decreased by 1.2 kg/m^3 at 1 µs, which corresponds to the temperature change of 1.02 K.

In the spectroscopic results, it was claimed that the isomer was formed after prompt photodissociation and survived up to few µs [7,8]. To check the possibility of isomer formation, we separately performed the global-fitting using the isomer formation reaction. The χ^2 value for the model including the isomer formation process (25.96) was greater than that without it (2.809) as in Fig. 2(A) by 9 folds at 10 ns time-delay. More importantly, if we include the isomer formation channel and let it float in the fitting process, the fraction of isomer formation converged to zero. These findings confirm that the dissociation channel without the isomer formation reproduces the experimental difference diffraction curves with higher reliability than does the model including the isomer formation channel.

ACKNOWLEDGMENTS

REFERENCES

1. P. Allen and D. J. Tildesley, *Computer Simulation of Liquids*, Clarendon Press: Oxford, 1989.
2. A, Plech et al., *Phys. Rev. Lett.* **92**, 125505 (2004).
3. M. Wulff et al., *J. Chem. Phys.* **124**, 034501 (2006).
4. H. Ihee et al., *Science* **124**, 1223-1227 (2005).
5. Kim et al., *Proc. Natl. Acad. Sci.* accepted for publication (2006).
6. M. Saes, *Phys. Rev. Lett.* **90**, 047403 (2003).
7. M. Wall et al., *J. Phys. Chem. A* **107**, 211-217 (2003).
8. X. Zheng and D. L. Phillip, *Chem. Phys. Lett.* 324, 175-180 (2000).
9. M. Cammarata et al., *J. Chem. Phys.* **124**, 124504 (2006).
10. S. Aditya and J. E. Willard, *J. Am. Chem. Soc.* **79**, 2680-2681 (1957).